

# BedSAT: Antarctica

Exploring what lies beneath using big data and modelling

Ana Fabela Hinojosa<sup>1</sup>  
September, 2025

Supervisors:  
Dr. Felicity McCormack  
Dr. Jason Roberts  
Dr. Richard Jones

Panel:  
Dr. Fabio Capitanio (Chair)  
Dr. Andrew Gunn  
Dr. Ariaan Purich



MONASH University



---

<sup>1</sup>[ana.fabelahinojosa@monash.edu](mailto:ana.fabelahinojosa@monash.edu)

## **Impact Statement**

Antarctica's bed topography data currently has local uncertainties of hundreds of metres in elevation due to sparse and unevenly distributed radar surveys, significantly limiting our ability to predict ice sheet behaviour and sea level rise contributions. Through the BedSAT project, I am developing a novel modelling approach that integrates remote sensing data and airborne-derived estimates, with mathematical and numerical ice flow models to substantially improve bed topography resolution and accuracy. I aim to derive a continent-wide bed topography dataset and conduct sensitivity analyses of dynamic ice loss to different realisations of topographic roughness through 2300CE. My work will quantify how bed topography uncertainties affect ice mass loss projections. This improved understanding can provide more reliable sea level rise predictions, and enable evidence-based policy decisions for climate adaptation strategies. This open-source approach and FAIR data principles will ensure these improvements benefit the broader scientific community and support more effective climate change mitigation planning.

# Contents

<b>1</b>	<b>TODO list</b>	<b>4</b>
<b>2</b>	<b>Antarctica's Landscape</b>	<b>5</b>
2.1	Climate Impacts and Global Significance . . . . .	5
<b>3</b>	<b>Topography of Antarctica</b>	<b>6</b>
3.1	Approaches to Bed Topography Reconstruction . . . . .	6
3.1.1	Ancient Landscapes Preserved Beneath the Ice Sheet . . . . .	8
3.2	Theoretical Frameworks . . . . .	9
3.2.1	Ice Flow Over Bedrock Perturbations - Budd 1970 . . . . .	9
3.2.2	Ice flow perturbation analysis - Ockenden 2023 . . . . .	10
3.2.3	Bridging Classical and Modern Approaches . . . . .	10
3.3	Current Opportunities . . . . .	11
<b>4</b>	<b>Methods</b>	<b>12</b>
4.1	Aims . . . . .	12
4.2	Research plan methodology . . . . .	12
4.2.1	Foundational Analysis of Bed-to-Surface Signal Transfer . . . . .	12
4.2.2	Development of the BedSAT Inversion Framework . . . . .	13
4.2.3	Derive a new bed topography for Antarctica using BedSAT . . . . .	13
4.2.4	Evaluate the impact of the improved bed topography . . . . .	13
<b>5</b>	<b>Progress</b>	<b>14</b>
5.1	Writing Contributions . . . . .	14
5.1.1	Synthetic bed topographies for Antarctica and their utility in ice sheet modelling . . . . .	14
5.1.2	SMUG . . . . .	15
5.2	Recreating ISMIP-HOM . . . . .	15
5.2.1	Transient evolution ISMIP-HOM . . . . .	18
5.3	Rheology and Sliding Study . . . . .	18
5.3.1	Non-Linear Rheology for Exp F . . . . .	19
5.3.2	The Current Computational Framework of this Study . . . . .	22
5.3.3	Ice Flow Simulation . . . . .	22
5.3.4	Data Processing and Visualization Tools . . . . .	23
5.3.5	Scientific Analysis Tools . . . . .	24
5.4	Current Conclusions . . . . .	28

# TODO list

1. Complete the missing literature review section
2. Add interpretation of phase analysis results: Given current findings (what does this mean for my inversion approach???) An isolated bump differs from the 90° prediction. Because the derivation in the Budd's 1970 is based on a periodic, harmonic bedrock (continuous, infinitely repeating cosine wave). The bump in IsmipF is a fundamentally different geometry. It does not have a single wavelength and introduces edge effects not accounted for in this periodic model. I want to include a periodic cosine wave to test budd more directly but the simulations are tricky (need to figure out correct resolution factors)
3. HOW CAN I USE the sliding study in the inversion method?
  - different transfer functions for different rheological assumptions?
  - test which rheology best matches observed data?
4. Consider whether timeline is realistic or if scope adjustment is needed
5. Include more discussion of limitations and potential challenges

# Antarctica's Landscape

## 2.1 Climate Impacts and Global Significance

The polar regions are losing ice, and their oceans are changing rapidly [1]. The consequences of this extend to the whole planet and it is crucial for us to understand them to be able to evaluate the costs and benefits of potential mitigation. Changes in different kinds of polar ice affect many connected systems. Of particular concern is the accelerating loss of continental ice sheets (glacial ice masses on land) in both Greenland and Antarctica, which has become a major contributor to global sea level rise [1]. Impacts extend beyond direct ice loss: as fresh water from melting ice sheets is added into the ocean, it increases ocean stratification disrupting global thermohaline circulation [2]. In addition, cold freshwater can dissolve larger amounts of CO<sub>2</sub> than regular ocean water creating corrosive conditions for marine life [1]. While there is high confidence in current ice loss and retreat observations in many areas, there is more uncertainty about the mechanisms driving these changes and their future progression [3]. Uncertainty increases in regions with variable bed conditions, where characteristics like bed slipperiness and roughness are difficult to verify via direct observations. Other problematic areas involve the ice sheet grounding line (GL): The zone that delineates ice grounded on bedrock from ice shelves floating over the ocean. The GL retreat rate depends crucially on topographical features like pinning points [3], which lead to increased buttressing by the ice shelf on the upstream ice sheet. Although this mechanism is established, major knowledge gaps persist in mapping bed topography across Antarctic ice sheet margins, with over half of all margin areas having insufficient data within 5 km of the grounding zone [4]. Addressing this data gap through both systematic mapping and improved interpolation —utilising auxiliary data streams with more complete coverage— would significantly improve both our understanding of current ice dynamics and the accuracy of ice-sheet models projecting future changes.

# Topography of Antarctica

Bed topography is one of the most crucial boundary conditions that influences ice flow and loss from the Antarctic Ice Sheet (AIS) [5]. Bed topography datasets are typically generated from airborne radar surveys, which are sparse and unevenly distributed across the Antarctic continent (see figure 3.1). Interpolation schemes to “gap fill” these sparse datasets yield bed topography estimates that have high uncertainties (i.e. multiple hundreds of metres in elevation uncertainty; Morlighem et al., 2020) which propagate through simulations of AIS evolution under climate change [6]. Given the logistical challenges of accessing large parts of the Antarctic continent, there is a crucial need for alternative approaches that integrate diverse and possibly more spatially complete data streams – including satellite data.

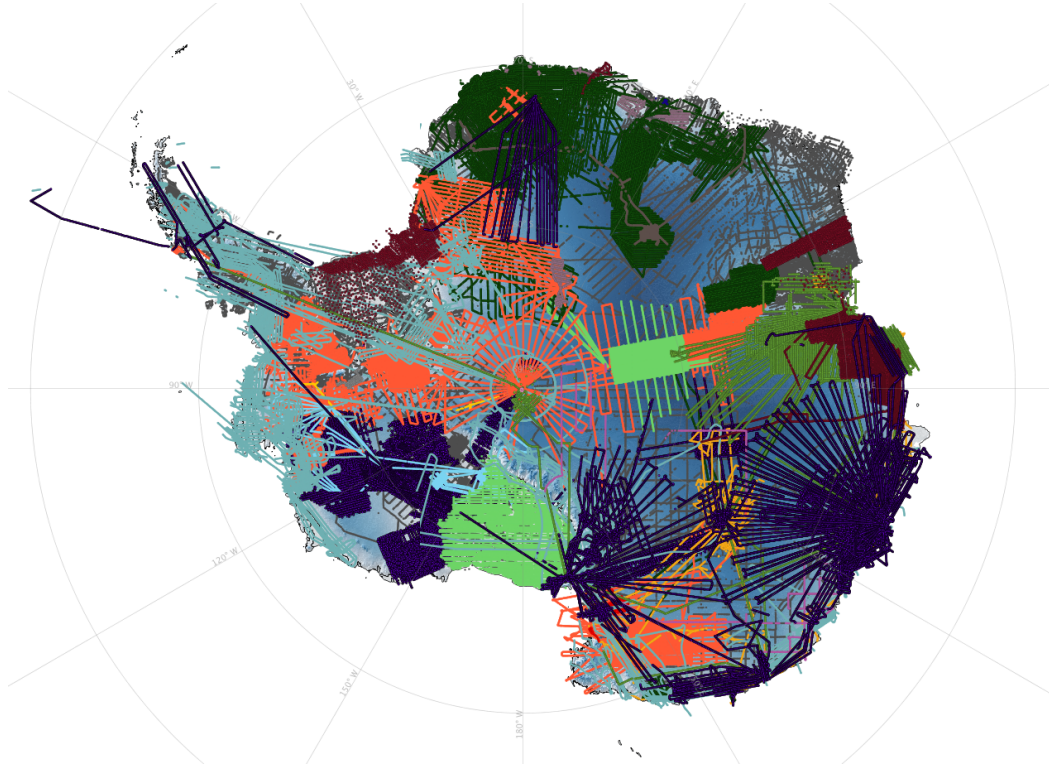


**Figure 3.1:** Distribution of BedMAP{1,2,3} data tracks (Source: [bedmap.scar.org](http://bedmap.scar.org)).

## 3.1 Approaches to Bed Topography Reconstruction

An objective of my research is to understand the bed topography itself and how it influences ice dynamics. There are two ways to infer information about this relationship:

Through forward modelling, with assumptions of the bed conditions; and through inverse modelling that relies on surface observations.

- **Forward models**

The aim of forward models is to see how bed properties impact ice dynamics. A key example is using a large ensemble of bed topographies to investigate how bed uncertainties impact simulated ice mass loss. Geostatistical methods can be used to generate bed topographies that either preserve elevation or texture:

- **Geostatistics** is comprised of statistical methods specialized for analyzing spatially correlated data. In glaciology, this approach is used to interpolate between sparse measurements and characterise spatial patterns in bed properties, often employing techniques like kriging [7] or flexural modeling—a computational method that models the earth’s lithosphere response to addition or removal of materials—See subsection 3.1.1 for more information on this technique.

- **Inversion models**

The aim of these models is to understand bed properties through knowledge of surface or other variables. A key example is the retrieval of bed topography or basal slipperiness from surface elevation and velocities.

- **Control method inversion:** A variational approach that minimizes mismatches between observed and simulated fields through a cost function approach. Remote sensing data and theoretical ice flow models are used to obtain basal conditions [8]. Often needs regularization terms to prevent non-physical features or over-fitting [9].
- **4dvar:** Four-dimensional variational data assimilation - Similar to the control method inversion algorithm, but adds a time dimension. Used to optimize model parameters and initial conditions [9]. Can handle time-varying data and evolving glacier states, making it more suitable for dynamic systems unlike control methods, this makes them more computationally demanding [9].
- **Mass conservation:** Used to constrain inversion models and fill data gaps by employing physical conservation laws, particularly effective for reconstructing bed topography where direct measurements are sparse [5, 10]. Requires (contemporary) measurements of ice thickness at the inflow boundary to properly constrain the system [9].
- **Markov Chain Monte Carlo (MCMC):** A probabilistic method that generates sample distributions to quantify uncertainties in ice sheet parameters and models [9]. While powerful for uncertainty quantification, these methods remain computationally intensive for continental-scale ice sheet models [9].
- **EnKF Ensemble Kalman Filter.** A sequential data assimilation method that uses an ensemble of model states to estimate uncertainty and update model parameters based on observations [9].

Despite revolutionary advances in satellite technology that provide unprecedented surface detail, a key challenge in glaciology remains: how to fully utilize this wealth of information in regions where our understanding of subglacial conditions is limited. My research aims to develop an integrated method combining forward and inverse modeling to improve bed

topography estimates by leveraging high-resolution satellite surface data in regions where radar data is sparse.

### 3.1.1 Ancient Landscapes Preserved Beneath the Ice Sheet

Discoveries of landscapes preserved beneath the Antarctic Ice Sheet provide crucial context and motivation for developing new bed reconstruction methods. Jamieson et al., (2023) identified a hidden river landscape ( $\approx 32,000 \text{ km}^2$  total area, with 800 m mean relief) under the ice in central east Antarctica. The preserved landscape was mapped using a combined data stream approach that incorporates satellite (RADARSAT, REMA) and Radar Echo Sounding (RES) data. Their approach—using ice surface slope changes to infer buried topography—exemplifies how multiple data integration can be leveraged to develop bed topography mappings beneath the ice sheet. The methods used by Jamieson et al. (2023) offer a direct template for BedSAT’s methods and validation. To test their hypothesis of an ancient land surface preserved beneath the modern EAIS, the researchers established a set of criteria (relevant anywhere in the continent) to be met by their observations. The geostatistical techniques they used include

- Flexural modeling In the form of isostatic rebound (uplift) modeling they demonstrate how the landscape responds when the ice removes material via erosional unloading. The paper shows that the current landscape is consistent with a splitting of a single uplifted topographic feature.
- Hypsometric distributions which demonstrated that the region investigated actually satisfied a common elevation signature.
- quantitative analysis This work provides a real-world quantitative target for what high-resolution bed topography should look like in this region. They identify a mean relief of  $\approx 800\text{m}$  and ridge-valley spacings of 2 to 3 km. This provides a crucial benchmark for my work with BedSAT. I aim to reproduce similar physically realistic statistical properties.

The paper arguments on landscape preservation strongly motivate the rheology and sliding conditions analysis in my own work (see Section 5.3). Since there are dramatic differences in the landscape expression depending on whether there is sliding conditions or not at the base of a glacier. Jamieson et al. find that rapid transitions between warm-based (erosive) and cold-based (preservative) ice states are necessary to explain the landscape’s survival. The paper argues that the landscape predates 14 Ma (and possibly 34 Ma), this implies that there is long-term thermal stability over these blocks of ancient terrain, with cold-based ice being the average glacial condition since landscape formation [11]. Their conclusion that the ice margin has not retreated this far inland for at least 14 Ma provides a critical long-term stability benchmark , reinforcing the need for improved bed topography models to accurately project how this stability may change under future anthropogenic climate forcing.

## 3.2 Theoretical Frameworks

Understanding how bed features manifest in surface observations requires a theoretical framework that connects these two domains. The modelling approach used in this project relies on two different theoretical frameworks that relate bed topography and surface features. Using synthetic data, observations and these modelling frameworks, my goal is understanding the limitations of each approach and how they can be improved.

### 3.2.1 Ice Flow Over Bedrock Perturbations - Budd 1970

The first framework was originally developed by Budd [12]. This model relates ice flow over bedrock perturbations to surface expressions using a two-dimensional biharmonic stress equation. The modelling carried out by Budd determined ice-sliding velocities for wide ranges of roughness, normal stress, and shear stress relevant to real glaciers [12]. Budd's framework fits in my project as a means of verifying the validity of the physics in my ice-sheet model, since it describes important effects of bedrock disturbances on the transient evolution of the transferred basal disturbances onto the surface. The theory makes several key predictions that have been confirmed through spectral analysis of real ice cap profiles:

1. A wavelength of minimum damping occurs at approximately 3.3 times the ice thickness,
2. surface undulations exhibit a  $\pi/2$  phase lag relative to bedrock features with steepest surface slopes occurring over the highest bedrock points, and
3. the amplitude reduction depends systematically on ice speed, viscosity, thickness, and wavelength.

Importantly, Budd's theory demonstrates that energy dissipation and basal stress patterns are maximized for bedrock irregularities with wavelengths several times the ice thickness, while smaller-scale bedrock variations decay exponentially with distance into the ice and have minimal impact on overall ice motion. This selective filtering of bedrock signals provides crucial insights for understanding which scales of bed topography most significantly influence ice dynamics. A critical aspect of Budd's theoretical framework is understanding how ice rheology affects the bed-to-surface transfer relationships. Glen's flow law typically employs a stress exponent  $n \approx 3$  for ice under most natural conditions, reflecting the strongly nonlinear relationship between stress and strain rate. Budd's analysis revealed that under certain low-stress conditions, ice deformation can behave more linearly ( $n \approx 1$ ) than conventional wisdom suggests. This rheological distinction has profound implications for bed-to-surface transfer functions: because linear rheology ( $n = 1$ ) may produce different amplitude dampening and phase relationships compared to nonlinear rheology ( $n = 3$ ), particularly for wavelengths around the critical 3.3 times ice thickness scale. My current modelling work systematically explores this by generating forward models for multiple synthetic bedrock profiles across four scenarios combining rheological assumptions ( $n = 1$  vs  $n = 3$ ) with basal boundary conditions (no-slip vs sliding), enabling direct comparison of how these physical assumptions affect the detectability and reconstruction of bed features from surface observations. Understanding these differences is essential for developing robust inversion methods, as the choice of rheological model fundamentally determines the mathematical relationship between observable surface expressions and the

underlying bed topography I seek to reconstruct. Crucially, Budd's work established the concept of frequency-dependent transfer functions that act as "filters" between bed and surface topography. This transfer function approach, expressed as  $\psi(\omega) = \frac{\text{surface amplitude}}{\text{bed amplitude}}$  for wavelength  $\lambda = 2\pi/\omega$ , provides a direct mathematical framework for inversion. By inverting these transfer functions, one can theoretically reconstruct bed topography from surface observations, particularly for wavelengths where the damping factor is minimal and the signal-to-noise ratio is optimal.

### 3.2.2 Ice flow perturbation analysis - Ockenden 2023

The second framework in my analysis builds upon these foundational concepts through some of the recent work by Ockenden et al. in [13], which uses observed surface perturbations (in velocity and elevation) to invert for unknown basal perturbations. Ockenden et al. improve from their previous work in [14] by using full-Stokes transfer functions, which greatly improves their method when dealing with steep topography where the shallow-ice-stream approximation breaks down. Ockenden et al. find this is crucial for better resolving the topographic features they are interested in. The core principle of the method by Ockenden et al. (2023) relies on the fact that variations in basal topography, slipperiness, and roughness cause measurable disturbances to the surface flow of the ice. Through linear perturbation analysis, they establish a systematic relationship between surface observations and bed conditions. This relationship can be expressed as  $y = f(x)$ , where  $y$  represents surface measurements (velocity and topography),  $x$  represents bed properties (topography and slipperiness), and  $f$  is the forward model transfer function refined by Gudmundsson and Raymond in 2008 [15]. In their work Ockenden et al apply this framework in reverse  $x = f^{-1}(y)$ , to infer the bedrock from modern, high-resolution satellite data estimates. A restrictive assumption in the modeling design by Ockenden et al might be their assumption of "constant viscosity", in glaciology this is equivalent to assuming a linear rheology, where the stress exponent,  $n$ , is equal to 1. This means that the strain rate is directly proportional to the stress. This is in contrast to the more commonly used non-linear Glen's Flow Law, where  $n$  is typically around 3 or even 4. This earliest phase in my PhD project has as a goal to determine whether treating the rheology of ice as linear is adequate. Ockenden et al account for a non-linear sliding law at the base of the ice, mentioning the "sliding law parameter m". However, the transfer of stress through the body of the ice—the core of the perturbation analysis—relies on the constant viscosity assumption from the foundational work of Gudmundsson and Raymond 2008.

### 3.2.3 Bridging Classical and Modern Approaches

While both frameworks address the fundamental bed-to-surface relationship, they operate at different levels of complexity and make different assumptions. Budd's approach provides the fundamental physical understanding of how specific wavelengths propagate through ice, establishing theoretical limits on what bed features can be detected from surface observations. Ockenden's method extends this to practical applications using real satellite data but relies on linearised assumptions that may break down under certain conditions. My research aims to bridge these approaches by combining Budd's rigorous transfer function analysis with comprehensive forward modeling that relaxes some of the restrictive assumptions inherent in linear perturbation methods. By systematically exploring how different rheological models ( $n = 1$  vs  $n = 3$ ) and basal conditions affect

the bed-to-surface transfer functions, my work aims to develop a robust inversion method that can better handle the nonlinear physics of ice flow while maintaining the theoretical rigor established by Budd's foundational analysis.

### 3.3 Current Opportunities

Current Antarctic bed topography reconstruction methods fail to utilize the wealth of presently available satellite-derived surface data. While mathematical models linking bed to surface through ice dynamics (such as those by Ockenden and Budd) provide a foundation for inferring bed topography from satellite data, they have significant limitations. My approach with BedSAT builds upon theoretical foundations and recent inversion methods to better understand how bed conditions—including slipperiness, roughness, and pinning points—affect both grounding line retreat rates and their surface expressions. BedSAT will connect surface observations with bed topography using more realistic rheological and geometric assumptions through an iterative process: initially inverted bed topography will feed into ice dynamics models with these improved assumptions, allowing comparison between model predictions and established datasets like NASA's ITS\_LIVE. I expect to utilise Machine learning methods to systematize this process, enhancing the analytical capabilities for the project's final phase.

# Methods

## 4.1 Aims

My research plan is structured around these three broad research questions:

1. How does the bed topography manifest on the ice surface?
2. To what extent do interpolation uncertainties in bed topography datasets affect the accuracy of Antarctic Ice Sheet evolution simulations under different climate change scenarios?
3. What is the impact of variable bed conditions and topography on the rate of grounding line (GL) retreat in continental ice sheets?

Underpinning these research questions are the following objectives (O):

- O1: Develop an ice sheet modelling approach to assimilate satellite remote sensing datasets to improve knowledge of the bed (BedSAT) informed by mathematical models of ice flow over topography;
- O2: Derive a new bed topography for Antarctica using BedSAT;
- O3: Evaluate the impact of the improved bed topography on projections of ice mass loss from Antarctica under climate warming through sensitivity analyses.

## 4.2 Research plan methodology

In order to achieve these objectives, each will be addressed in sequential phases. My primary focus is currently on O1: Deriving the BedSAT method. As the initial phase of O1, I am working on an investigation on the influence of different combinations of rheological and sliding law assumptions in ice sheet modeling. The goal of this investigation is to systematically understand the forward problem —how the bed affects the surface under different physical rules— to then use that knowledge to build a better inverse model (BedSAT).

### 4.2.1 Foundational Analysis of Bed-to-Surface Signal Transfer

The first critical step is to systematically quantify how fundamental physical assumptions influence the expression of subglacial topography at the ice surface. This directly addresses my first research question: "How does the bed topography manifest on the ice surface?".

This work will leverage the Ice-sheet and Sea-level System Model (ISSM) with a custom-built computational framework based on a synthetic bed topography database. This systematic study will verify and validate the necessary set of constraints on bed-to-surface transfer functions that account for realistic ice dynamics.

#### 4.2.2 Development of the BedSAT Inversion Framework

By understanding how rheology and sliding conditions alter the surface expression of the bed, I can develop more physically robust transfer functions for the inversion process. The inversion model will be developed and tested using a regional catchment in Antarctica with extensive radar data, such as the Aurora Subglacial Basin (this data can be found in works such as [16]). The model will be constrained by available observations of surface velocity, thermal distribution, and ice thickness, this will allow for direct validation of the inversion results against known bed configurations. Furthermore, the robustness of the model will be ensured through grid independence testing and a sensitivity analysis of model assumptions. See Chapter 5 for detailed information on the progress of this work.

#### 4.2.3 Derive a new bed topography for Antarctica using BedSAT

I will apply the validated BedSAT methodology from O1 to the entire Antarctic continent, deriving a new continent-wide bed topography dataset. Using covariance properties from existing radar surveys, I will generate multiple realisations of the bed, each with unique and statistically-consistent topographic roughness.

#### 4.2.4 Evaluate the impact of the improved bed topography

The new bed topography datasets will be used to conduct a sensitivity analysis of ice sheet model projections to 2300 CE. This will investigate the impact of the improved topography and different roughness realisations on ice dynamics, subglacial hydrology, and overall ice mass loss from Antarctica, directly addressing the project's main research questions.

*Note: Detailed methodological outlines for O2 and O3 will be developed following the completion and refinement of the BedSAT method in O1.*

# Progress

## 5.1 Writing Contributions

### 5.1.1 Synthetic bed topographies for Antarctica and their utility in ice sheet modelling

I contributed to the investigation and writing of the manuscript titled “Synthetic bed topographies for Antarctica and their utility in ice sheet modelling,” which has been submitted to the journal Proceedings of the Royal Society A. This comprehensive review and case study examines the various methods used to generate synthetic bed topographies for Antarctica, assessing their underlying objectives, associated uncertainties, and their impact on ice sheet model projections of sea level rise. My contribution was focused on the literature review of key methodologies used to generate these topographies. I was responsible for authoring the descriptions for several prominent techniques, including:

- Mass Conservation: Detailing how this physics-informed approach, as implemented in widely-used datasets like BedMachine [5] and the TELVIS algorithm [17], is used to reconstruct bed topography by ensuring the continuity of ice volume across the glacial system.
- Ensemble Kalman Filter (EnKF): Summarising this data assimilation technique which uses an ensemble of model states to estimate and update system parameters based on new observations, thereby tracking the transient evolution of an ice sheet. Some relevant works include [18, 19].
- Linear Perturbation Theory: Referenced works using this method are included and discussed in section 3.2 of this report.

By describing these distinct approaches, their physical assumptions, and their limitations, my work helped to establish the theoretical context for the paper’s case study on the Aurora Subglacial Basin. This review framed the comparison between different types of synthetic beds ("elevation-preserving" vs. "texture-preserving") and underscored how methodological choices in bed generation can significantly influence projections of future sea level contributions

### 5.1.2 SMUG

I have also contributed to the investigation and writing of a manuscript detailing a new interpolation method for sparse and unevenly sampled data. The manuscript is titled: "Antarctic bed topography estimation using a Stochastic Meshless Uncertainty Gridding (SMUG) method". This manuscript will be submitted to Elsevier. My contribution involved conducting a review of existing interpolation techniques helping to author the introductory section of the manuscript. My writing establishes the scientific context and rationale for the development of SMUG. I analysed several established methods used in previous Antarctic bed topography datasets, including:

- Inverse Distance Weighting (IDW): Used in Bedmap1 [20], a straightforward method that can produce overly smooth surfaces and struggle with highly variable data.
- Kriging: A geostatistical method that provides uncertainty estimates but often requires subjective, expert-driven parameter selection, which can introduce bias. This method is evaluated in Bedmap2 [21] and Bedmap3 [22] and found to produce less accurate results than other methods such as spline interpolation.
- Spline Interpolation (e.g., Topogrid): The key technique in Bedmap2 [21], this method demonstrated good performance but faced challenges in optimising smoothing parameters and honouring all data points.
- Mass Conservation Methods: Implemented in BedMachine [5], this physics-informed approach improves accuracy in data-sparse regions but requires additional datasets (like ice velocity) that are not always available.

Through my investigation, I identified and articulated key limitations and research gaps inherent in these widely-used techniques. Specifically, my writing highlighted the common difficulties in providing robust uncertainty estimates, avoiding systematic biases, and capturing the spatial correlation of errors realistically. This analysis sets the stage for the manuscript to introduce SMUG as a method designed to overcome these specific shortcomings, setting the foundation upon which the novelty and significance of the SMUG method were demonstrated in our manuscript.

## 5.2 Recreating ISMIP-HOM

As a first step in validating the computational framework for this project and to build a understanding foundation of the capabilities and functionality of ISSM, I replicated a series of benchmark experiments from the Ice Sheet Model Intercomparison Project for Higher-Order Models (ISMIP-HOM) [23]. Successfully replicating these benchmarks demonstrates that the simulation setup is configured accurately capturing the fundamental physics of ice flow. Part of my recreation focused on the first four diagnostic experiments (A, B, C, and D), which test a model's ability to simulate ice flow under a range of conditions. Experiments A and B involve flow over a sinusoidally varying bed topography (a "bumpy" 3D bed and a "rippled" 2D bed, respectively) with no basal sliding. These experiments are designed to evaluate the model's handling of longitudinal and vertical stress gradients induced by basal topography. Conversely, Experiments C and D feature a flat bed but introduce spatially variable basal friction, simulating the dynamics of an

ice stream with slippery and sticky patches. All my models utilised full-Stokes equations (FS).

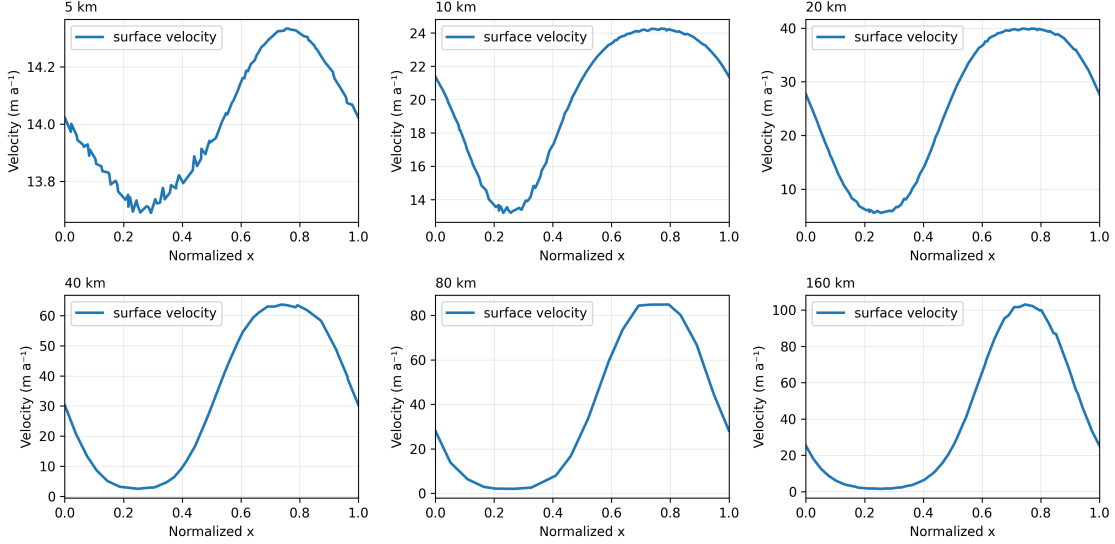


**Figure 5.1:** ISSM recreation of ISMIP-HOM Experiment A: Ice flow over a bumpy bed. The panels show the the surface velocity for a 3D ice flow simulation over a sinusoidal bed with no basal sliding ( $v_b = 0$ ). Each panel corresponds to a different domain length scale (L), from 5 km to 160 km.

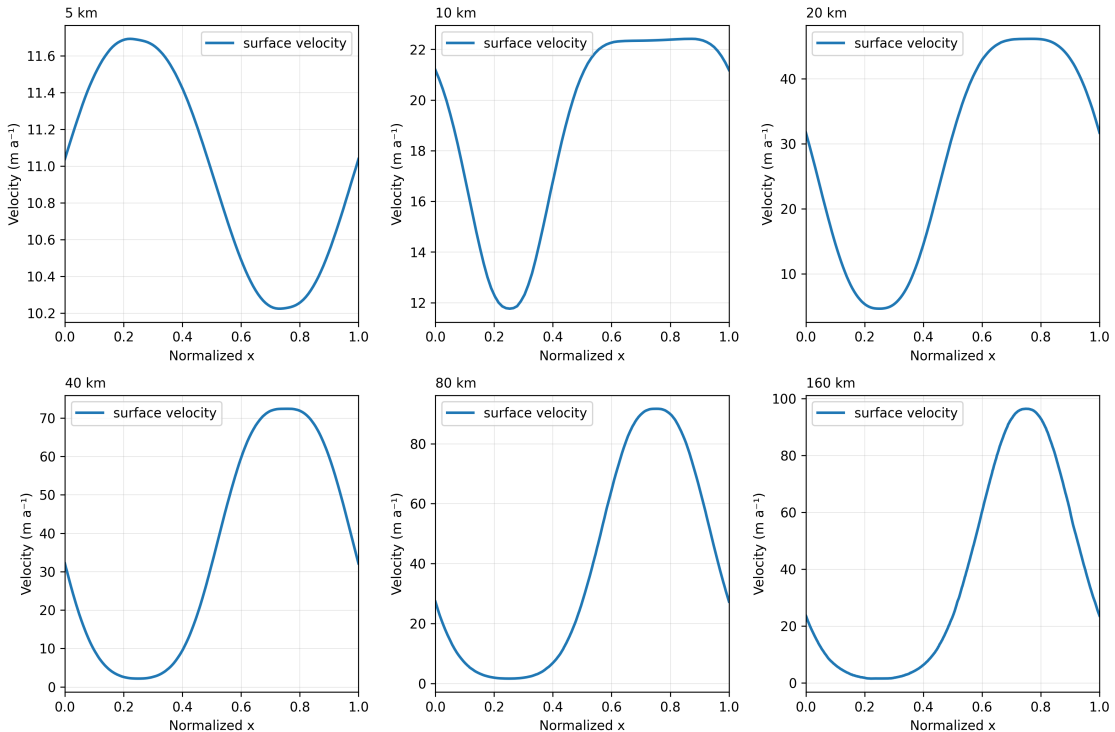


**Figure 5.2:** ISSM recreation of ISMIP-HOM Experiment B: Ice flow over a rippled bed. The panels show the surface velocity for a 2D flowline simulation. The setup is identical to Experiment A, but the basal topography does not vary in the y-direction, isolating longitudinal stress effects.

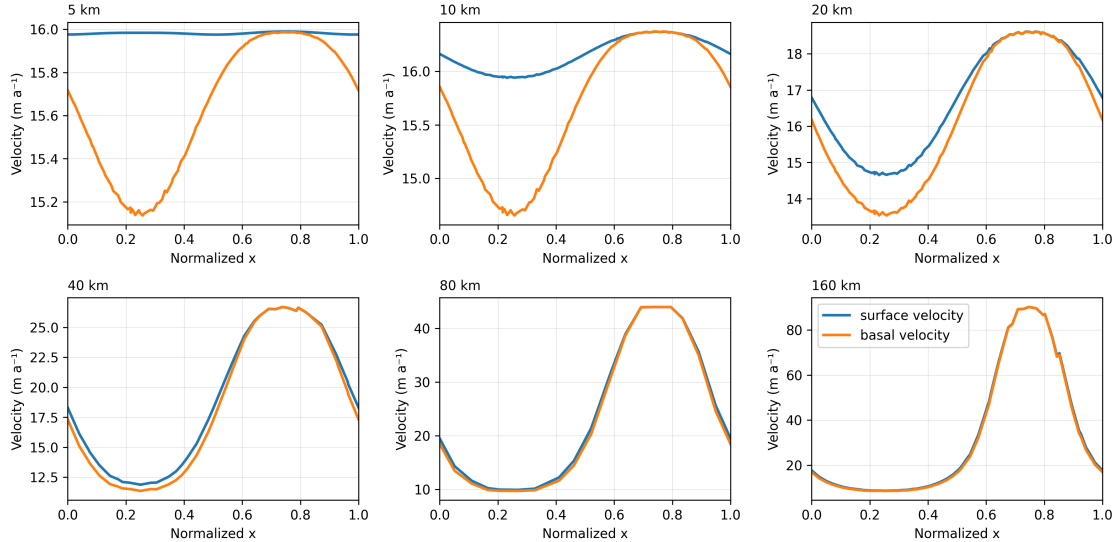


**Figure 5.3:** ISSM recreation of ISMIP-HOM Experiment C: Ice stream flow I. The panels show both surface (blue) and basal (orange) velocity for a 3D simulation over a flat bed where basal motion is governed by a spatially variable friction coefficient,  $\beta^2(x, y)$ .

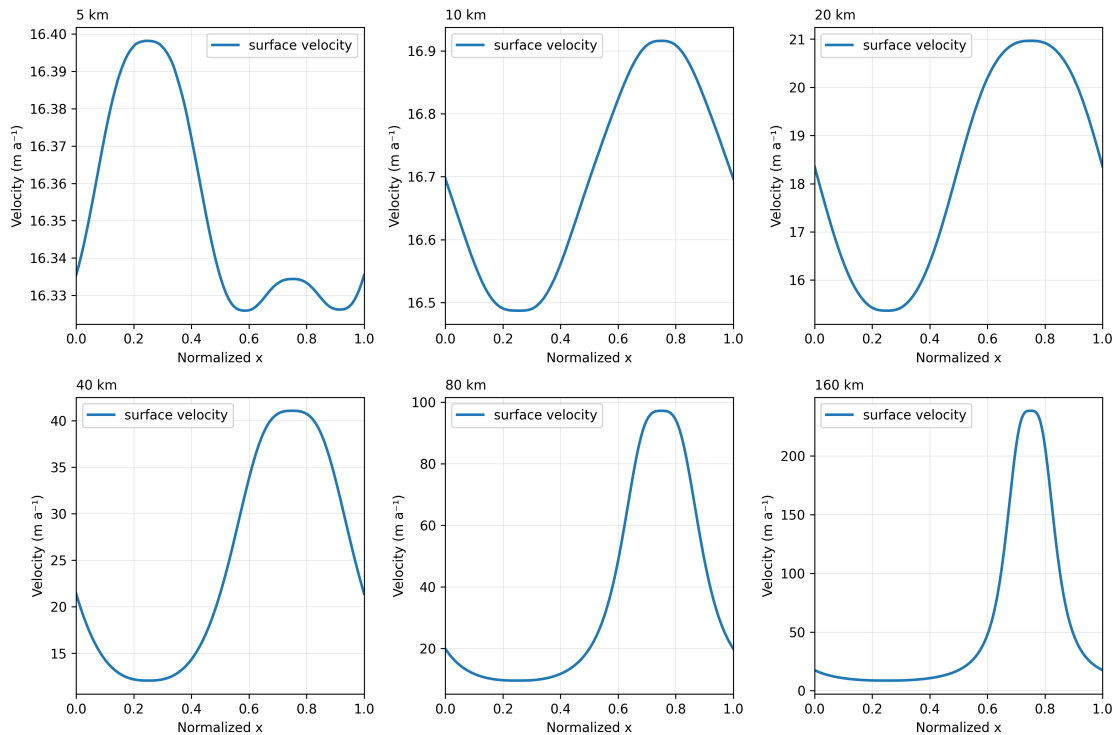


**Figure 5.4:** ISSM recreation of ISMIP-HOM Experiment D: Ice stream flow II. The panels show the surface velocity for a 2D flowline over a flat bed with variable basal friction. The setup is identical to Experiment C, but the friction coefficient varies only in the x-direction,  $\beta^2(x)$ .

The results from these simulations demonstrate a strong agreement with the published findings in [23]. For all experiments and across the different prescribed length scales ( $L = 5 \text{ km}$  to  $160 \text{ km}$ ), the calculated surface velocities closely matched the behaviour of the full-Stokes (FS) models from the original ISMIP-HOM. My results show the same effects as the original ISMIP HOM. Smaller length scale experiments demonstrate a decreased velocity amplitude, likely due to the ice undergoing a form of viscous drag, rather

than being influenced by the individual bedrock undulations. This successful validation confirms that my computational framework is robust and reliably simulates complex ice dynamics. This verification establishes a solid foundation for the application of my framework to more complex simulation settings and its subsequent research questions. In subsection 5.2.1 I work on extending the findings in Pattyn et al, 2008. To investigate the transient (Prognostic) experiment F where the free surface is allowed to relax until a steady state is reached for zero surface mass balance [23]

### 5.2.1 Transient evolution ISMIP-HOM

Building upon the diagnostic ISMIP-HOM experiments, this work extends the prognostic experiment F to systematically investigate the combined effects of rheology and basal sliding within a benchmark ice sheet model. The original experiment F included two scenarios: one with a frozen bed (no-slip) and another with linear sliding. My study expands upon these conditions by also incorporating non-linear rheology. This addition generates four distinct scenarios for comparison:

- S1 No-slip (frozen) bed + Linear rheology ( $n = 1$ ).
- S2 No-slip (frozen) bed + Non-linear rheology ( $n = 3$ ).
- S3 Linear sliding + Linear rheology ( $n = 1$ ).
- S4 Linear sliding + Non-linear rheology ( $n = 3$ ).

While the original study by Pattyn et al. (2008) covered scenarios S1 and S3, understanding the impact of rheological assumptions is crucial for modern ice sheet modelling. During periods of rapid grounding line retreat, uncertainty in the Glen flow law exponent  $n$  has been found to cause a larger spread in ice-loss projections than uncertainty in climate forcing [24]. Therefore, explicitly testing these different physical conditions is a critical step. This foundational analysis, validated against a well-established benchmark, will provide the necessary confidence in the modelling framework before extending the work to a suite of more complex synthetic bed topographies.

## 5.3 Rheology and Sliding Study

This study forms the core of my 'Foundational Analysis of Bed-to-Surface Signal Transfer' as outlined in Section 4.2.1. The objective here is to move beyond theoretical concepts and systematically quantify how fundamental physical assumptions—specifically ice rheology and basal conditions alter the expression of subglacial topography at the ice surface. I isolate the impact of these assumptions in a controlled setup. The results from this analysis will directly inform the BedSAT framework. Budd's sliding theory describes stress propagation through flowing ice over undulating bedrock. The stress field propagates upward at an angle, creating surface (elevation) waves that are phase-shifted by approximately  $\pi/2$  relative to bedrock (elevation) features, in Budd's words: '**the maximum shear stress occurs at the tops of the waves and the minimum in the troughs**' [12]. My work up until now has been focused in building a comprehensive computational framework developed for the systematic investigation of ice dynamics. The first part of this framework is to study via flow simulations the behavior of ice to understand the relationship between

basal geometry, ice rheology, and overall flow response. A key objective of this work is to understand the effect of commonly made assumptions in ice sheet modelling and their repercussions for the validity of the resulting models. This initial stage is designed to be a complete, end-to-end pipeline, from environment setup to final scientific analysis.

### 5.3.1 Non-Linear Rheology for Exp F

This rheology study directly addresses a critical gap in current inversion methods. While approaches like Ockenden et al. (2023) assume linear rheology ( $n = 1$ ), my results (see Figures 5.5 and 5.6) demonstrate that non-linear rheology produces substantially different bed-to-surface transfer characteristics. These findings will enable BedSAT to incorporate rheology-dependent transfer functions, potentially improving bed topography reconstruction accuracy in regions where non-linear ice behavior dominates. In order to extend Experiment F in Pattyn et al., (2008) ISMIP-HOM to encompass non-linear rheology and still be consistent, I must ensure that different model rheologies start from identical initial conditions. The method I follow here is based on re-scaling method by Getraer and Morlighem (2025) [24]. Their formula ensures that the initial ice viscosity—and therefore strain rates for a given stress—is identical between simulations with different rheologies.

The fundamental model for the deformation of glacial ice and the equations which govern ice flow is Glen's flow law.

$$\dot{\varepsilon} = A_n \tau^n, \quad (5.1)$$

We can also write Glen's flow law in terms of the material's resistance to deformation—the viscosity—which is not a constant value but changes depending on stress and strain rates.

$$\tau = 2\mu \dot{\varepsilon}, \quad (5.2)$$

which means that  $A^{-1/n} = 2\mu \dot{\varepsilon}^{\frac{n-1}{n}}$ , where  $B = A^{-1/n}$  (Pa s<sup>1/n</sup>) is an alternative formulation of the rate factor known as the rigidity. The rigidity parameter is commonly used in ISSM to characterise the rheology of ice in a model. This is the parameter that will be scaled. The definition of ice viscosity uses the rigidity; for any  $n > 0$ :

$$\mu_n = \frac{B_n}{2 \dot{\varepsilon}^{\frac{n-1}{n}}}, \quad (5.3)$$

setting the viscosity as equal for both linear and non-linear rheology scenarios implies that the strain rates can be set as equivalent between linear and non-linear rheology scenarios

$$\mu_1 = \frac{B_1}{2}, \quad (5.4)$$

Then setting  $\mu_1 = \mu_n$  and rearranging for  $B_n$

$$\frac{B_1}{2} = \frac{B_n}{2 \dot{\varepsilon}^{\frac{n-1}{n}}} \quad (5.5)$$

Letting  $n = 1$ , this means we are treating ice a Newtonian fluid (viscosity is independent to changes in stress). Since  $B_1 = A^{-1}$  where value of  $A_1$  is taken as from Pattyn (2008).

$$B_1 = (2.14037310^{-7})^{-1} \text{ Pa a}, \quad (5.6)$$

For the non-linear scenarios I am considering  $n = 4$ , since the assumption of  $n = 3$  for ice deformation is not universally supported and values of  $n > 3$  have been inferred from

real-world glaciers. Suggesting that a value of  $n = 4$  better represents the actual behavior of glaciers in some places [24]. Then scaling the rigidity for the non-linear scenarios is:

$$B_4 = B_1 \dot{\varepsilon}^{\frac{4-1}{4}} = B_1 \dot{\varepsilon}^{\frac{3}{4}}, \quad (5.7)$$

Here the strain rate is the characteristic strain rate that can be derived from the unperturbed velocity. For simple shear,  $\dot{\varepsilon} \approx U/H$ . Where  $U$  is the mean ice velocity and  $H$  is the ice thickness. From the grid convergence analyses in 5.3.5, I discovered that the highest grid resolution ( $2.0 \times 2.0$ ) converges to velocities  $U_{S1} = 102.75 \text{ m a}^{-1}$  and  $U_{S3} = 205.09 \text{ m a}^{-1}$  for the frozen and sliding scenarios respectively. The ice thickness is  $H = 1000 \text{ m}$ , therefore the characteristic strain rate for S1 is  $\dot{\varepsilon}_{S1} = 0.10275 \text{ a}^{-1}$ . Leaving the scaled rigidity for the frozen bed and non-linear rheology experiment (S2) as,

$$B_4 = B_1 \dot{\varepsilon}_{S1}^{\frac{3}{4}}. \quad (5.8)$$

While for S3 the characteristic strain rate is  $\dot{\varepsilon}_{S3} = 0.20509 \text{ a}^{-1}$ . Therefore, the scaled rigidity for the sliding and non-linear rheology experiment S4 is

$$B_4 = B_1 \dot{\varepsilon}_{S3}^{\frac{3}{4}}. \quad (5.9)$$

The resultant surface elevations and velocities after a 300 year transient evolution For the frozen and sliding bed scenarios are

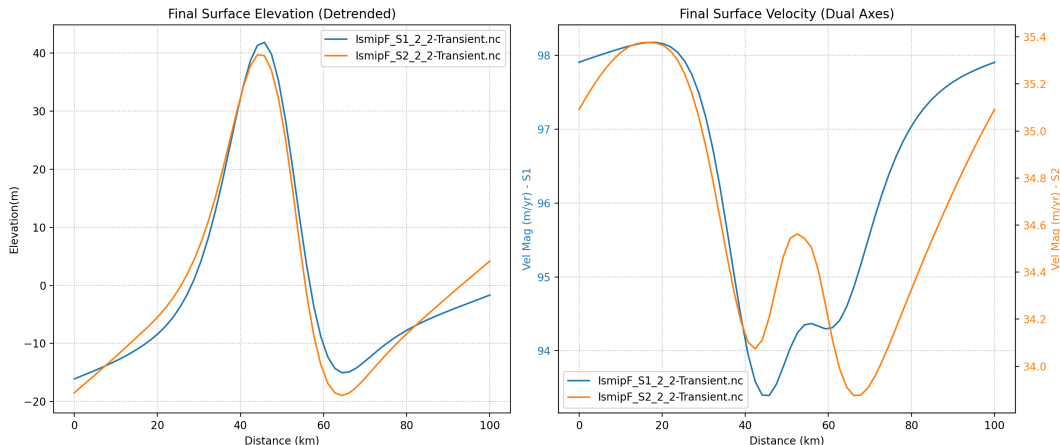


**Figure 5.5:** Final surface elevations and velocities for the original frozen bed Experiment F (S1) and the corresponding transformed to non-linear rheology experiment (S2)

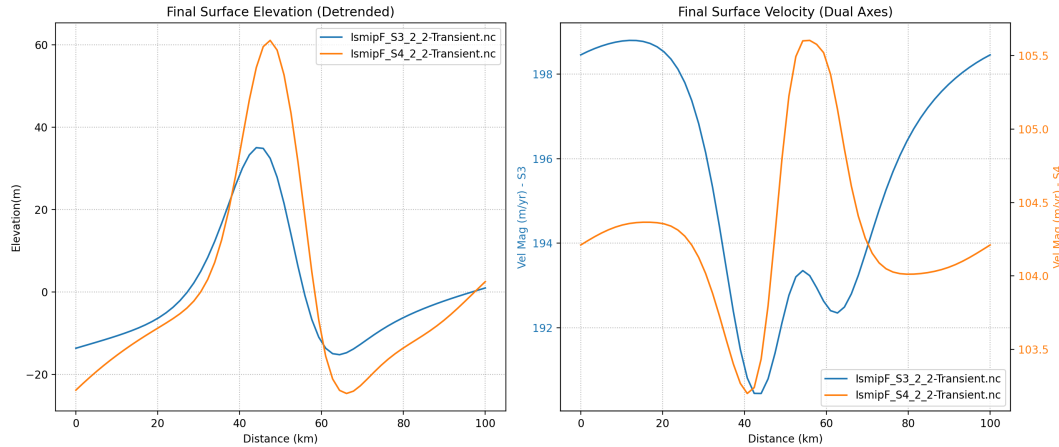


**Figure 5.6:** Final surface elevations and velocities for the original sliding bed Experiment F (S3) and the corresponding transformed to non-linear rheology experiment (S4)

These results are consistent with the surface elevation and velocities found by Pattyn et al., (2008) for Exp. F—along the central flowline of the domain—for the both the frozen and sliding experiments. The non-linear scenarios(S2 and S4) shown in orange in Figures 5.6 and 5.5 represent the first key finding of this foundational analysis. The marked differences in both final surface elevation and velocity compared to the linear counterparts (S1, S3) provide crucial evidence for my first research question (“How does the bed topography manifest on the ice surface?”). The ice viscosity and hence its deformation is directly influenced by the stress and strain according to Glen’s flow law. Given the power law relationship, using an  $n = 4$  exponent leads to a strong non-linear relationship where a small increase in stress yields a much larger increase in deformation. This becomes visible as more complex flow adjustments—ice becomes softer in high stress regions and stiffer in low stress ones—in the non-linear models. These results demonstrate that the choice of rheology is not a minor parameter choice, but a control on the bed-to-surface signal transfer. It is necessary to address the nuance from these results given that while non-linear rheology better represents ice physics, this study’s aim is to quantify whether this increased realism improves bed topography reconstruction accuracy enough to justify the additional computational complexity in the inversion framework. An important benefit that could come from realistic rheology assumptions in models is that they could theoretically produce surface patterns that better match satellite observations, potentially improving inversion accuracy. The next stage in this investigation is developing a variety of synthetic bedrock topographies to understand the relationship between basal geometry, ice rheology, and overall flow response to more complex bed conditions.

### 5.3.2 The Current Computational Framework of this Study

This study is supported by a suite of interconnected scripts and tools designed for generating conditions, running simulations, processing output, and performing scientific analysis.

### 5.3.3 Ice Flow Simulation

The core of this study is a time evolution flow simulation of fully grounded ice over 300 years with daily time steps. This simulation is designed to systematically investigate the relationship between basal geometry, ice rheology and flow response by running a series of ISMIP-HOM style experiments [23] that can later be analysed in detail with other data processing tools 5.3.4. The simulations solve Higher order (HO) ice flow equations for a static diagnostic stress balance and a transient run (which includes stress balance and mass transport configurations). The simulation utilises periodic boundary conditions which represents a section of an infinitely long ice sheet effectively eliminating edge effects that would arise from standard inlet/outlet boundaries. The script couples the inlet and outlet velocities by matching vertices in the base layer and then extruding this setup vertically. This ensures that the ice flow is continuous and that the dynamics are driven solely by the underlying topography and internal stresses, which is crucial for studying the transfer of bedrock signals to the surface. This approach has proved to be highly successful, yielding stable and physically realistic velocities across experimental scenarios. The results are consistent with established benchmarks like ISMIP-HOM and show the expected physical relationships (e.g., faster flow with sliding and non-linear rheology). The experimental design tests different physical conditions being built around four benchmark experiments from subsection 5.2.1. The simulation friction parameters are identical to those set in Pattyn et al., (2008) which themselves follow the scaling given by Gudmundsson (2003), where the basal friction coefficient is related to the slip ratio  $c$  by

$$\beta^2 = (cAH)^{-1} \quad (5.10)$$

Where S1, S2 utilise a frozen bed condition ( $c = 0$ ) while S3, S4 utilise a sliding bed ( $c = 1$ ). The main simulation scripts produce .nc files and binary .outbin files for full simulation results (when run locally and on the NCI Gadi system respectively). The simulation framework in this study includes capabilities for systematic grid convergence testing, comparing solutions across multiple mesh resolutions to ensure the results are independent of the mesh discretisation, (see Section 5.3.5).

### 5.3.4 Data Processing and Visualization Tools

I have developed a set of robust, high-performance scripts to handle the large volume of data produced by the ice flow simulations. (Note that: All batch scripts have their individual file processing counterpart)

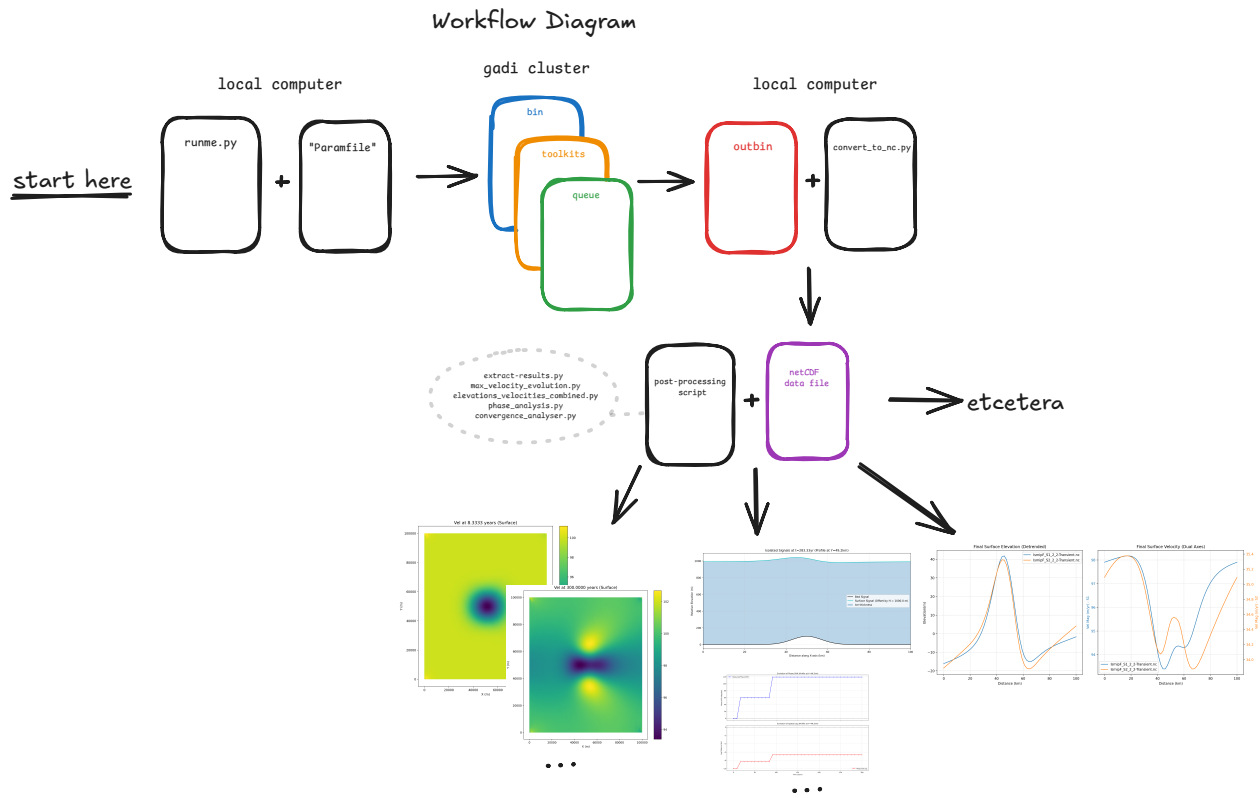


**Figure 5.7:** Diagrammatic representation of the current workflow using my ice simulation and analysis suite. For a particular simulation I will extract the results and visually inspect the output using all analysis scripts in the suite.

1. Binary to NetCDF Conversion A batch-capable tool (`batch_convert.py`) converts ISSM .outbin files into the standard, portable NetCDF format. This script supports parallel processing for high throughput.
2. Result Extraction and Visualization A batch script (`batch_extract_results.py`) that automatically finds and processes NetCDF files to generate visualisations of key fields like velocity and pressure.
3. Targeted Scientific Plotting Additional scripts are used to create specific scientific plots.

As per Figure 5.7, my workflow requires more automation. I still need to develop tools to do most of the post processing analysis in the cluster. This is a work in progress.

### 5.3.5 Scientific Analysis Tools

#### Grid Independence

In order to perform quantitative analysis on the simulation results. I developed a convergence analysis script: `convergence_analyser.py`. Grid convergence analysis is a fundamental verification technique in computational modeling that ensures numerical solutions are approaching the true solution as mesh resolution increases. The key principle is that as the grid is refined (smaller elements, more nodes), the numerical error should decrease systematically. The grid analysis involved running simulations across 16 distinct mesh resolutions, generated by independently varying both the horizontal ( $H$ ) and vertical ( $V$ ) grid densities. Note that I have kept the vertical layer thickness constant. I applied resolution scaling factors of 2.0 i.e. double the resolution, 0.5 i.e. half the mesh resolution, 1.0 i.e. no scaling and 1.5 i.e. 50% scaling. I designated the solution from the highest resolution mesh, corresponding to scaling factors of ( $H = 2.0, V = 2.0$ ) as the reference solution against which all coarser meshes were compared. Refined meshes (either horizontal or vertical) often require smaller time steps to satisfy the Courant-Friedrichs-Lowy (CFL) condition and maintain solver stability. To satisfy this criterion I scaled the time step for each simulation matching the largest resolution factor independently if it was horizontal or vertical scaling. The primary metric of this script is the L2 relative error, a global, scale-dependent measure that quantifies the overall difference between two solutions. In my analysis, I chose a convergence threshold of 1%—since estimates of other uncertainties are expected to be larger than grid errors—when comparing the solutions to the baseline. If the L2 norm of the data is very close to zero (less than  $10^{-6}$ ), the analysis reports the absolute error to avoid division by a tiny, unstable number. Otherwise, it calculates and reports the standard relative error as a percentage. The `convergence_analyser.py` script generates a standardised  $2 \times 2$  plot (see figures 5.8, 5.9, 5.10, 5.11) to provide a comprehensive view of convergence via L2 error bars, and the maximum velocity at every time step. In addition the output plot shows visual velocity comparisons along a centre line in the  $y$  dimension. This is done for surface and basal velocities for each mesh resolution tested. The code identifies all unique  $y$ -coordinates present in the mesh layer (surface or base) then finds the  $y$ -coordinate that is numerically closest (given some threshold) to the defined geometric centre line, then it selects all nodes whose  $y$ -coordinate matches this identified “closest”  $y$ -coordinate. The script effectively extracts the entire mesh line closest to the ideal centre for each simulation. The code also establishes a reference grid based on the baseline resolution chosen, then sorts and interpolates the velocity data based on this reference grid iteratively for all resolutions, the script interpolates the sorted velocity data for each resolution onto the common reference grid.

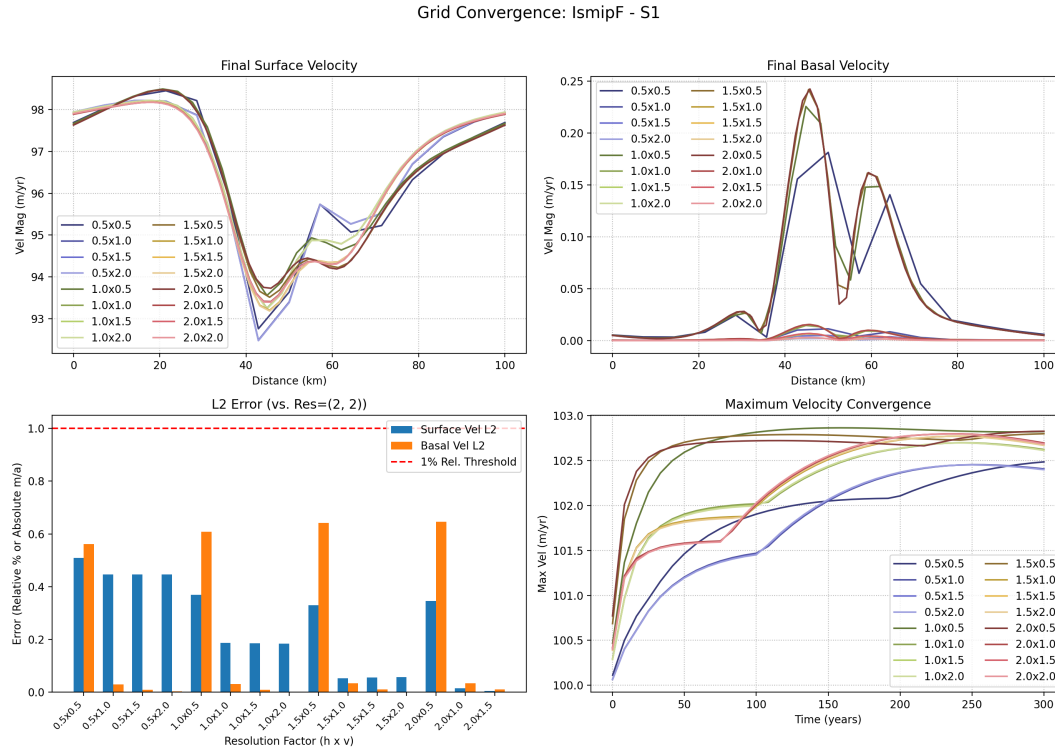


**Figure 5.8:** Grid convergence analysis for Scenario S1 (frozen bed, linear rheology,  $n = 1$ ). The four panels show: (top-left) final surface velocity profiles and (top-right) final basal velocity profiles for 16 different mesh resolutions; (bottom-left) the L2 relative error of each simulation compared to the highest-resolution mesh ( $2.0 \times 2.0$ ), with a 1% relative error threshold indicated by the dashed line; and (bottom-right) the evolution of the maximum velocity over the 300-year simulation period

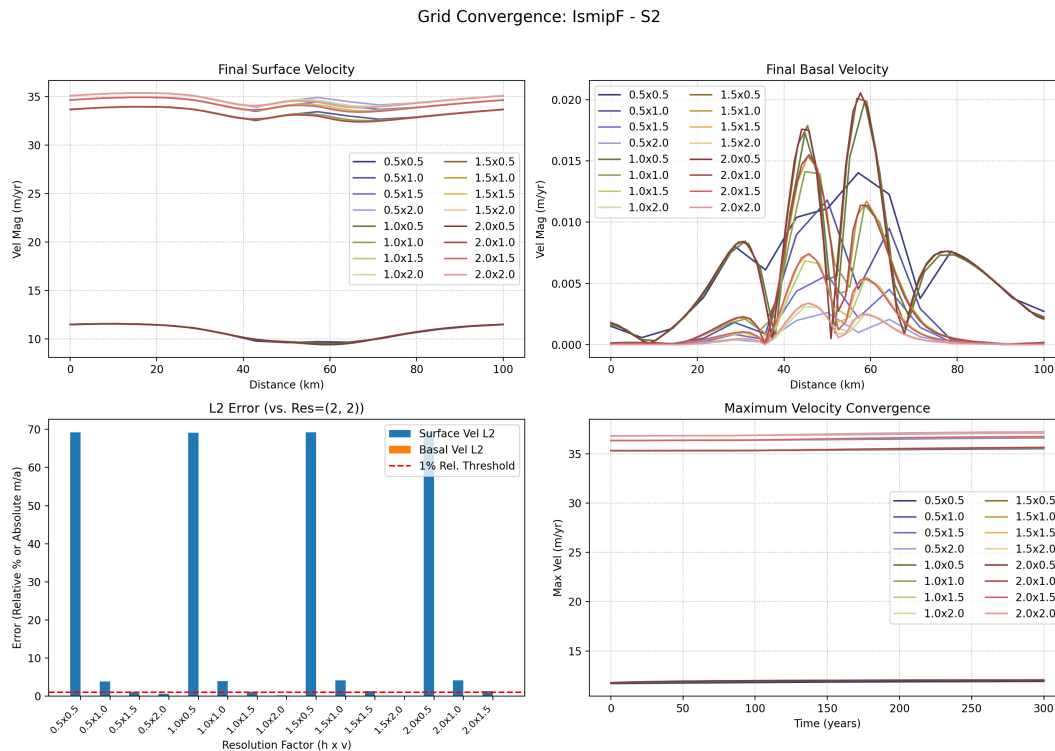


**Figure 5.9:** Grid convergence analysis for Scenario S2 (frozen bed, non-linear rheology,  $n = 4$ ). An extension of ISMIP-HOM Experiment F. The panels display the same metrics as Figure 5.8. This scenario exhibits high sensitivity to vertical resolution refinement, with low-resolution simulations showing the highest errors and converging to a much slower flow state ( $\approx 11$  m/a) compared to high-resolution runs ( $\approx 37$  m/a).

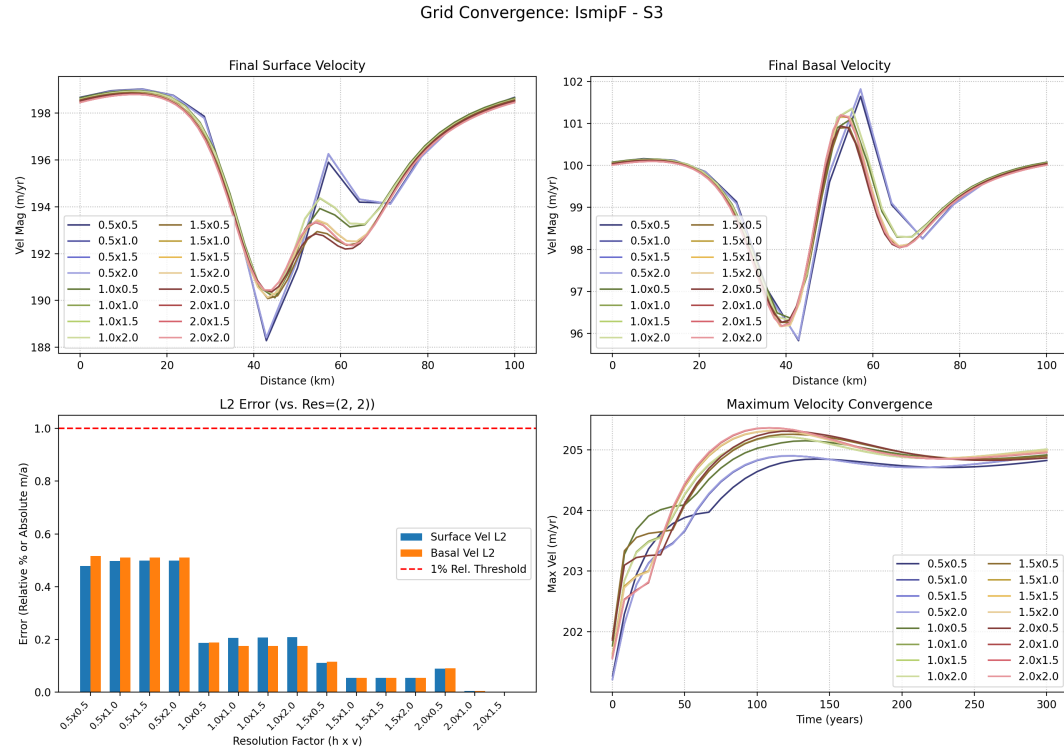


**Figure 5.10:** Grid convergence analysis for Scenario S3 (linear sliding, linear rheology,  $n = 1$ ). The four panels show: (top-left) final surface velocity profiles and (top-right) final basal velocity profiles for 16 different mesh resolutions; (bottom-left) the L2 relative error of each simulation compared to the highest-resolution mesh ( $2.0 \times 2.0$ ), with a 1% relative error threshold indicated by the dashed line; and (bottom-right) the evolution of the maximum velocity over the 300-year simulation period

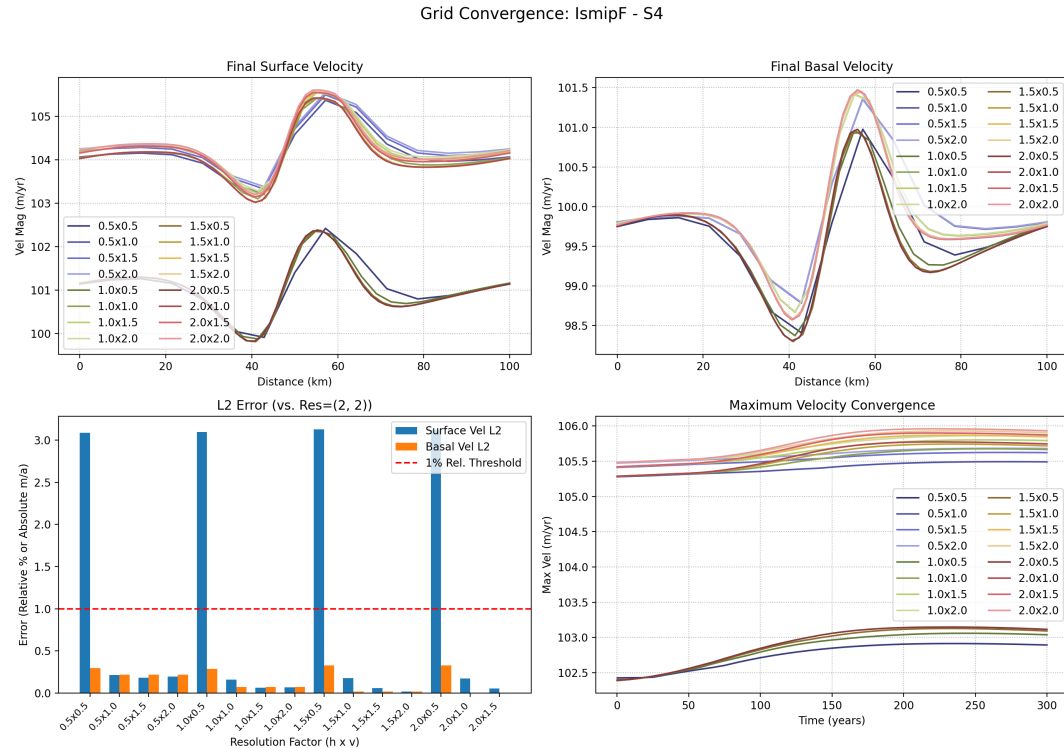


**Figure 5.11:** Grid convergence analysis for Scenario S4 (linear sliding, non-linear rheology,  $n = 4$ ). Another extension of ISMIP-HOM Experiment F, similarly to the other non-linear case (S2) in Figure 5.9, this scenario is highly sensitive to vertical resolution. The convergence analysis shows that the 1% relative error threshold is only achieved for simulations using the highest vertical resolution factor (2.0)

My diagnostic convergence analyses show that the simulations are most sensitive to vertical resolution refinement. The effect is more dramatic with the non-linear rheology scenarios in Figures 5.9 and 5.11. The convergence threshold of 1% is only achieved for both S2 and S4 with the vertical resolution factor 2.0. The vertical resolution of the mesh produces qualitatively different results as it is refined. The lowest vertical resolution simulations converge to a slow-flowing state ( $\approx 11\text{m/a}$ ). On the other hand the high-vertical resolution simulations converge to larger velocities ( $\approx 37\text{m/a}$ ). In addition to this, the Frozen bed scenario S2 basal velocities show the highest errors for low resolution simulations.

## Phase Analysis

I developed single and batch-processing scripts (e.g. `phase_analysis.py`) to directly quantify the the bed-to-surface phase signal transfer. This analysis provides a metric to verify that my model's physics are consistent with the criteria in [12]. Who predicted a phase shift of approximately  $\pi/2$ . My phase analysis tracks the evolution of the surface with respect to the base and uses cross-correlation to calculate the spatial lag and phase shift between the de-trended signals for each time step in a given simulation. The scripts generate time-series plots of phase shift evolution and summary text files with numerical results. For each batch or single simulation analysed. The code deduces key simulation parameters like the parameter profile, experimental scenario, and mesh resolution scaling factors from the name of the NetCDF script being analysed, then it configures and reconstructs the original model setup and mesh exactly as it was during the simulation run. For visualisation purposes, for each time step recorded in the NetCDF file the script extracts a 1D profile of the ice base and surface elevations along a user-defined line (e.g., along the x-axis at the domain's centre). The core of the analysis is to separate the "signal" (the topographic bump) from the "background" (the unperturbed, sloping ice sheet). It does this by calculating the theoretical baseline for the bed and surface and subtracting it from the actual elevations. To find the shift between the bedrock signal and the surface signal, the script uses cross-correlation (`scipy.signal.correlate`), the peak of this function corresponds to the spatial lag where the two signals are most similar. The spatial lag is converted into a phase shift in degrees using the bedrock's characteristic wavelength from the parameter file. These analysis steps are repeated for every time step in the simulation. The script stores the phase shift and lag distance for each point in time, allowing it to generate plots that show how the phase relationship evolves.

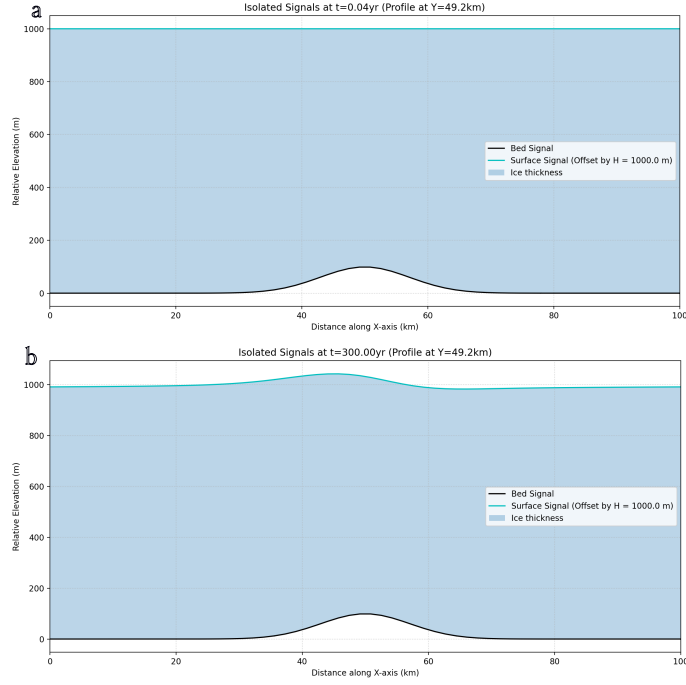


**Figure 5.12:** The isolated bedrock and ice surface signals (along the  $y$ - centreline) for the initial (a) and final (b) time steps in the 300 year long simulation. The bedrock is identical to that of ISMIP HOM experiment F (S1: Frozen bed and linear rheology). As time progresses and the ice surface responds to the underlying bed topography, the surface develops a bump that's spatially shifted relative to the bed bump (upstream due to ice flow dynamics).

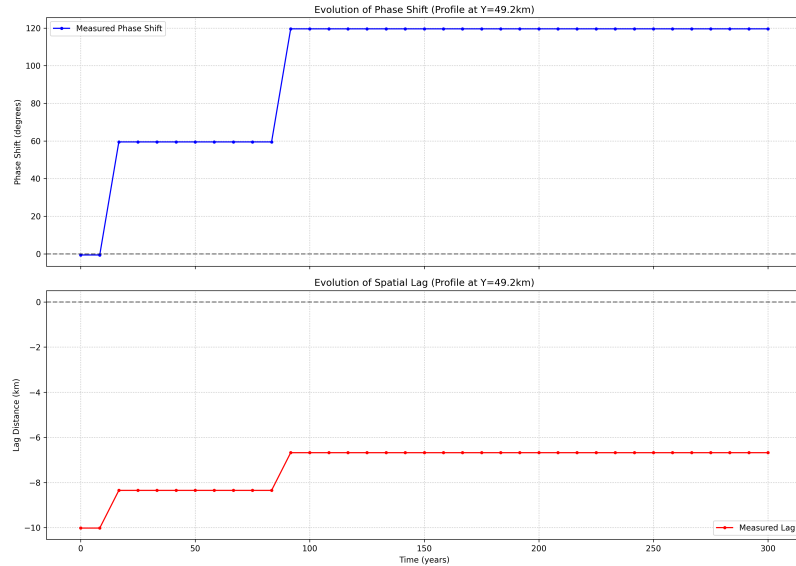
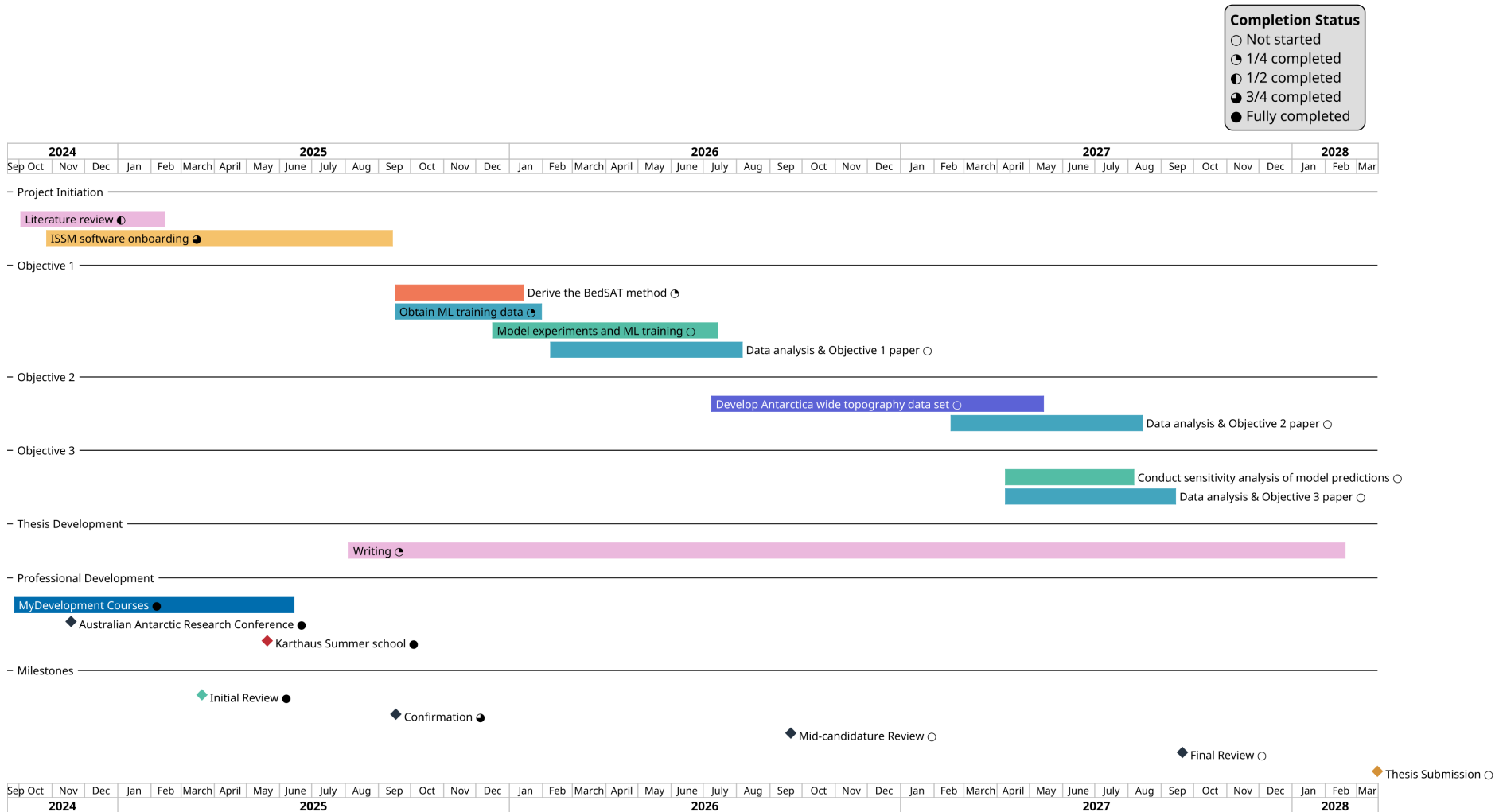


**Figure 5.13:** The evolution of the phase shift and spatial lag over the entire simulation.

The results for the phase analysis show that an isolated feature such as the Gaussian bump in Exp F in ISMIP-HOM produces a different phase shift ( $\approx \frac{2\pi}{3}$ ). This results highlights the limitations of applying Budd periodic theory to non-periodic features.

## 5.4 Current Conclusions

# Project timeline



# Bibliography

- [1] M. Meredith, M. Sommerkorn, S. Cassotta, C. Derksen, A. Ekaykin, A. Hollowed, G. Kofinas, A. Mackintosh, J. Melbourne-Thomas, M. M. C. Muelbert, G. Ottersen, H. Pritchard, and E. A. G. Schuur. *The Ocean and Cryosphere in a changing climate*, pages 203—320. Cambridge University Press, Cambridge, United Kingdom and New York, NY, USA (2019). DOI: [10.1017/9781009157964.005](https://doi.org/10.1017/9781009157964.005). 5
- [2] S. S. Jacobs. *Bottom water production and its links with the thermohaline circulation*. Antarctic Science **16**, 427–437 (2004). DOI: [10.1017/S095410200400224X](https://doi.org/10.1017/S095410200400224X). 5
- [3] B. Fox-Kemper, H. T. Hewitt, C. Xiao, G. Aðalgeirsdóttir, S. S. Drijfhout, T. L. Edwards, N. R. Golledge, M. Hemer, R. E. Kopp, G. Krinner, A. Mix, D. Notz, S. Nowicki, I. S. Nurhati, L. Ruiz, J.-B. Sallée, A. B. A. Slangen, and Y. Yu. *Ocean, Cryosphere and Sea Level Change*. In V. Masson-Delmotte, P. Zhai, A. Pirani, S. L. Connors, C. Péan, S. Berger, N. Caud, Y. Chen, L. Goldfarb, M. I. Gomis, M. Huang, K. Leitzell, E. Lonnoy, J. B. R. Matthews, T. K. Maycock, T. Waterfield, O. Yelekçi, R. Yu, and B. Zhou (editors), *Climate Change 2021: The Physical Science Basis. Contribution of Working Group I to the Sixth Assessment Report of the Intergovernmental Panel on Climate Change*, chapter 9, pages 1211–1362. Cambridge University Press, Cambridge, UK and New York, NY, USA (2021). DOI: [10.1017/9781009157896.011](https://doi.org/10.1017/9781009157896.011). 5
- [4] R. A. Group. *RINGS: Collaborative international effort to map all Antarctic ice-sheet margins*. Scientific Committee on Antarctic Research (2022). DOI: <https://doi.org/10.5281/zenodo.6638327>. 5
- [5] M. Morlighem, E. Rignot, T. Binder, D. Blankenship, R. Drews, G. Eagles, O. Eisen, F. Ferraccioli, R. Forsberg, P. Fretwell, V. Goel, J. S. Greenbaum, H. Gudmundsson, J. Guo, V. Helm, C. Hofstede, I. Howat, A. Humbert, W. Jokat, N. B. Karlsson, W. L. Lee, K. Matsuoka, R. Millan, J. Mouginot, J. Paden, F. Pattyn, J. Roberts, S. Rosier, A. Ruppel, H. Seroussi, E. C. Smith, D. Steinhage, B. Sun, M. R. van den Broeke, T. D. van Ommen, M. van Wessem, and D. A. Young. *Deep glacial troughs and stabilizing ridges unveiled beneath the margins of the Antarctic ice sheet*. Nature Geoscience **13**, 132 (2020). DOI: [10.1038/s41561-019-0510-8](https://doi.org/10.1038/s41561-019-0510-8). 6, 7, 14, 15
- [6] B. A. Castleman, N. J. Schlegel, L. Caron, E. Larour, and A. Khazendar. *Derivation of bedrock topography measurement requirements for the reduction of uncertainty in ice-sheet model projections of Thwaites Glacier*. The Cryosphere **16**, 761 (2022). DOI: [10.5194/tc-16-761-2022](https://doi.org/10.5194/tc-16-761-2022). 6
- [7] E. J. MacKie, D. M. S. J. Caers, M. R. Siegfried, and C. Scheidt. *Antarctic Topographic Realizations and Geostatistical Modeling Used to Map Sub-*

- glacial Lakes.* Journal of Geophysical Research: Earth Surface **125** (2020). DOI: <https://doi.org/10.1029/2019JF005420>. 7
- [8] J. D. Rydt, G. H. Gudmundsson, H. F. J. Corr, and P. Christoffersen. *Surface undulations of Antarctic ice streams tightly controlled by bedrock topography.* The Cryosphere **7**, 407 (2013). DOI: [10.5194/tc-7-407-2013](https://doi.org/10.5194/tc-7-407-2013). 7
- [9] M. Morlighem and D. Goldberg. *Data Assimilation in Glaciology*, pages 93–111. Cambridge University Press (2024). DOI: [10.1017/9781009180412.007](https://doi.org/10.1017/9781009180412.007). 7
- [10] M. Morlighem, C. N. Williams, E. Rignot, L. An, J. E. Arndt, J. L. Bamber, G. Catania, N. Chauché, J. A. Dowdeswell, B. Dorschel, I. Fenty, K. Hogan, I. Howat, A. Hubbard, M. Jakobsson, T. M. Jordan, K. K. Kjeldsen, R. Millan, L. Mayer, J. Mouginot, B. P. Y. Noël, C. O’Cofaigh, S. Palmer, S. Rysgaard, H. Seroussi, M. J. Siegert, P. Slabon, F. Straneo, M. R. van den Broeke, W. Weinrebe, M. Wood, and K. B. Zinglersen. *Bedmachine v3: Complete bed topography and ocean bathymetry mapping of greenland from multibeam echo sounding combined with mass conservation.* Geophysical Research Letters **44**, 11,051 (2017). ARXIV: <https://agupubs.onlinelibrary.wiley.com/doi/pdf/10.1002/2017GL074954>, DOI: <https://doi.org/10.1002/2017GL074954>. 7
- [11] S. Jamieson, N. Ross, G. Paxman, F. Clubb, D. Young, S. Yan, J. Greenbaum, D. Blankenship, and M. Siegert. *An ancient river landscape preserved beneath the East Antarctic Ice Sheet.* Nature Communications **14** (2023). DOI: [10.1038/s41467-023-42152-2](https://doi.org/10.1038/s41467-023-42152-2). 8
- [12] W. F. Budd. *Ice Flow Over Bedrock Perturbations.* Journal of Glaciology **9**, 29 (1970). DOI: [10.3189/S0022143000026770](https://doi.org/10.3189/S0022143000026770). 9, 18, 27
- [13] H. Ockenden, R. G. Bingham, A. Curtis, and D. Goldberg. *Ice-flow perturbation analysis: a method to estimate ice-sheet bed topography and conditions from surface datasets.* Journal of Glaciology **69**, 1677 (2023). DOI: [10.1017/jog.2023.50](https://doi.org/10.1017/jog.2023.50). 10
- [14] H. Ockenden, R. G. Bingham, A. Curtis, and D. Goldberg. *Inverting ice surface elevation and velocity for bed topography and slipperiness beneath Thwaites Glacier.* The Cryosphere **16**, 3867 (2022). DOI: [10.5194/tc-16-3867-2022](https://doi.org/10.5194/tc-16-3867-2022). 10
- [15] G. H. Gudmundsson and M. Raymond. *On the limit to resolution and information on basal properties obtainable from surface data on ice streams.* The Cryosphere **2**, 167 (2008). DOI: [10.5194/tc-2-167-2008](https://doi.org/10.5194/tc-2-167-2008). 10
- [16] D. A. Young, A. P. Wright, J. L. Roberts, R. C. Warner, N. W. Young, J. S. Greenbaum, D. M. Schroeder, J. W. Holt, D. E. Sugden, D. D. Blankenship, and T. D. van Ommen. *A dynamic early East Antarctic Ice Sheet suggested by ice-covered fjord landscapes.* Nature **474**, 72 (2011). DOI: <https://doi.org/10.1038/nature10114>. 13
- [17] J. L. Roberts, R. C. Warner, D. Young, A. Wright, T. D. van Ommen, D. D. Blankenship, M. Siegert, N. W. Young, I. E. Tabacco, A. Forieri, A. Passerini, A. Zirizzotti, and M. Frezzotti. *Refined broad-scale sub-glacial morphology of Aurora Subglacial Basin, East Antarctica derived by an ice-dynamics-based interpolation scheme.* The Cryosphere **5**, 551 (2011). DOI: [10.5194/tc-5-551-2011](https://doi.org/10.5194/tc-5-551-2011). 14

- [18] F. Gillet-Chaulet. *Assimilation of surface observations in a transient marine ice sheet model using an ensemble Kalman filter*. *The Cryosphere* **14**, 811 (2020). DOI: [10.5194/tc-14-811-2020](https://doi.org/10.5194/tc-14-811-2020). 14
- [19] Y. Choi, A. Petty, D. Felikson, and J. Poterjoy. *Estimation of the state and parameters in ice sheet model using an ensemble Kalman filter and Observing System Simulation Experiments*. *EGUphere* **2025**, 1 (2025). DOI: [10.5194/egusphere-2025-301](https://doi.org/10.5194/egusphere-2025-301). 14
- [20] M. B. Lythe and D. G. Vaughan. *BEDMAP: A new ice thickness and subglacial topographic model of Antarctica*. *Journal of Geophysical Research: Solid Earth* **106**, 11335 (2001). ARXIV: <https://agupubs.onlinelibrary.wiley.com/doi/pdf/10.1029/2000JB900449>, DOI: <https://doi.org/10.1029/2000JB900449>. 15
- [21] P. Fretwell, H. D. Pritchard, D. G. Vaughan, J. L. Bamber, N. E. Barrand, R. Bell, C. Bianchi, R. G. Bingham, D. D. Blankenship, G. Casassa, G. Catania, D. Callens, H. Conway, A. J. Cook, H. F. J. Corr, D. Damaske, V. Damm, F. Ferraccioli, R. Forsberg, S. Fujita, Y. Gim, P. Gogineni, J. A. Griggs, R. C. A. Hindmarsh, P. Holmlund, J. W. Holt, R. W. Jacobel, A. Jenkins, W. Jokat, T. Jordan, E. C. King, J. Kohler, W. Krabill, M. Riger-Kusk, K. A. Langley, G. Leitchenkov, C. Leuschen, B. P. Luyendyk, K. Matsuoka, J. Mouginot, F. O. Nitsche, Y. Nogi, O. A. Nost, S. V. Popov, E. Rignot, D. M. Rippin, A. Rivera, J. Roberts, N. Ross, M. J. Siegert, A. M. Smith, D. Steinhage, M. Studinger, B. Sun, B. K. Tinto, B. C. Welch, D. Wilson, D. A. Young, C. Xiangbin, and A. Zirizzotti. *Bedmap2: improved ice bed, surface and thickness datasets for Antarctica*. *The Cryosphere* **7**, 375 (2013). DOI: [10.5194/tc-7-375-2013](https://doi.org/10.5194/tc-7-375-2013). 15
- [22] H. D. Pritchard, P. T. Fretwell, A. C. Fremant, J. A. Bodart, J. D. Kirkham, A. Aitken, J. Bamber, R. Bell, C. Bianchi, R. G. Bingham, D. D. Blankenship, G. Casassa, K. Christianson, H. Conway, H. F. J. Corr, X. Cui, D. Damaske, V. Damm, B. Dorschel, R. Drews, G. Eagles, O. Eisen, H. Eisermann, F. Ferraccioli, E. Field, R. Forsberg, S. Franke, V. Goel, S. P. Gogineni, J. Greenbaum, B. Hills, R. C. A. Hindmarsh, A. O. Hoffman, N. Holschuh, J. W. Holt, A. Humbert, R. W. Jacobel, D. Jansen, A. Jenkins, W. Jokat, L. Jong, T. A. Jordan, E. C. King, J. Kohler, W. Krabill, J. Maton, M. K. Gillespie, K. Langley, J. Lee, G. Leitchenkov, C. Leuschen, B. Luyendyk, J. A. MacGregor, E. MacKie, G. Moholdt, K. Matsuoka, M. Morlighem, J. Mouginot, F. O. Nitsche, O. A. Nost, J. Paden, F. Pattyn, S. Popov, E. Rignot, D. M. Rippin, A. Rivera, J. L. Roberts, N. Ross, A. Ruppel, D. M. Schroeder, M. J. Siegert, A. M. Smith, D. Steinhage, M. Studinger, B. Sun, I. Tabacco, K. J. Tinto, S. Urbini, D. G. Vaughan, D. S. Wilson, D. A. Young, and A. Zirizzotti. *Bedmap3 updated ice bed, surface and thickness gridded datasets for Antarctica*. *Scientific Data* **12**, 414 (2025). DOI: [10.1038/s41597-025-04672-y](https://doi.org/10.1038/s41597-025-04672-y). 15
- [23] F. Pattyn, L. Perichon, A. Aschwanden, B. Breuer, B. de Smedt, O. Gagliardini, G. H. Gudmundsson, R. C. A. Hindmarsh, A. Hubbard, J. V. Johnson, T. Kleiner, Y. Konovalov, C. Martin, A. J. Payne, D. Pollard, S. Price, M. Rückamp, F. Saito, O. Souček, S. Sugiyama, and T. Zwinger. *Benchmark experiments for higher-order and full-Stokes ice sheet models (ISMIP-HOM)*. *The Cryosphere* **2**, 95 (2008). DOI: [10.5194/tc-2-95-2008](https://doi.org/10.5194/tc-2-95-2008). 15, 17, 18, 22

- [24] B. Getraer and M. Morlighem. *Increasing the Glen–Nye power-law exponent accelerates ice-loss projections for the Amundsen Sea Embayment, West Antarctica*. Geophysical Research Letters **52**, e2024GL112516 (2025). DOI: [10.1029/2024GL112516](https://doi.org/10.1029/2024GL112516).
- [18](#), [19](#), [20](#)